Brazilian Journal
of Chemical
Engineering

ISSN 0104-6632
Printed in Brazil
www.abeq.org.br/bjche

Vol. 31, No. 02, pp. 413 - 427, April - June, 2014
dx.doi.org/10.1590/0104-6632.20140312s00001956

NATURAL CONVECTION OF NANOFLUIDS OVER A CONVECTIVELY HEATED VERTICAL PLATE EMBEDDED IN A POROUS MEDIUM

M. Ghalambaz, A. Noghrehabadi* and A. Ghanbarzadeh

Department of Mechanical Engineering, Shahid Chamran University of Ahvaz, Ahvaz, Iran.
Phone: +98 611 3330010 Ext. 5678, Fax: +98 611 3336642.
E-mail: m.ghalambaz@gmail.com; E-mail: ghanbarzadeh.a@scu.ac.ir
*E-mail: noghrehabadi@scu.ac.ir

(Submitted: May 24, 2012 ; Revised: May 30, 2013 ; Accepted: July 5, 2013)

Abstract - In this paper, the natural convective flow of nanofluids over a convectively heated vertical plate in a saturated Darcy porous medium is studied numerically. The governing equations are transformed into a set of ordinary differential equations by using appropriate similarity variables, and they are numerically solved using the fourth-order Runge-Kutta method associated with the Gauss-Newton method. The effects of parametric variation of the Brownian motion parameter (*Nb*), thermophoresis parameter (*Nt*) and the convective heating parameter (*Nc*) on the boundary layer profiles are investigated. Furthermore, the variation of the reduced Nusselt number and reduced Sherwood number, as important parameters of heat and mass transfer, as a function of the Brownian motion, thermophoresis and convective heating parameters is discussed in detail. The results show that the thickness of the concentration profiles is much lower than the temperature and velocity profiles. For low values of the convective heating parameter (*Nc*), as the Brownian motion parameter increases, the non-dimensional wall temperature increases. However, for high values of *Nc*, the effect of the Brownian motion parameter on the non-dimensional wall temperature is not significant. As the Brownian motion parameter increases, the reduced Sherwood number increases and the reduced Nusselt number decreases.
Keywords: Nanofluid; Natural convection; Porous media; Thermophoresis; Brownian motion.

INTRODUCTION

The study of natural convection heat transfer in a porous medium is gaining a lot of attention because it has many engineering applications such as thermal energy storage, groundwater systems for industrial and agricultural use, flow through filtering media, and crude oil extraction (Gorla *et al*., 2011). The natural convection of pure fluids over embedded bodies has been analyzed in many previous studies. The free convection from a vertical plate with non-uniform surface temperature has been studied by Gorla and Zinalabedini (1987). Similarity solution of natural convection boundary layer flow along a vertical plate has been investigated by Cheng and Minkowycz (1977). Although the flow and heat transfer of natural convection over embedded bodies in porous media has been studied in a large number of papers, few papers have considered micro- and nanofluids.

Nanofluids are suspensions of submicron particles (nanoparticles) in a conventional fluid. The most important characteristic of nanofluids is their higher thermal conductivity relative to the base fluids, which can be achieved even at very low volume fractions of nanoparticles. In recent years, the heat transfer enhancement of nanofluids has been proposed as a route for surpassing the performance of heat transfer

*To whom correspondence should be addressed

rate in currently available liquids. The fluid containing nanoparticles can flow smoothly through microchannels without clogging them because they are small enough to behave similar to liquid molecules (Khanafer *et al.*, 2003). The unique property of nanofluids in enhancement of the heat transfer has attracted many researchers such as Hwang *et al*. (2009), Yu *et al*. (2008), and Daungthongsuk and Wongwises (2007) to investigate the heat transfer characteristics in nanofluids. Most researchers reported that the presence of the nanoparticles in the base fluid tremendously enhances the effective thermal conductivity of the fluid and consequently enhances the heat transfer characteristics. An excellent collection of articles on this topic can be found in Das *et al*. (2007), Wang *et al*. (2008a), Wang *et al*. (2008b), and Kakac and Pramuanjaroenkij (2009).

The current experimental results show that the forced and mixed convection enhancement can be achieved in the presence of nanoparticles, and this enhancement increases with the increase of the nanoparticle volume fraction (Hwang *et al*., 2009; Yu *et al*., 2008; Daungthongsuk and Wongwises, 2007). By contrast, experimental results show that in natural convection flow of nanofluids, the heat transfer coefficient decreases with an increase of the nanoparticle volume fraction (Putra *et al*., 2003; Nnanna, 2007; Wen and Ding, 2006; Chang *et al*., 2008). However, such agreement is not established, and there is a striking lack of experimental data for natural convection in both clear flows and flows in porous media (Polidori *et al*., 2007).

Recently, a large number of researchers have studied the convective heat transfer of nanofluids numerically including Nassan *et al*. (2010), Noghrehabadi *et al*. (2012c), Vajravelu *et al*. (2011), Wongcharee and Eiamsa-ard (2011), Yacob *et al*. (2011a), and Yacob *et al*. (2011b). Almost all of these researchers assumed that the nanofluid can be modeled as a common pure fluid (homogenous model), and the conventional equations of mass, momentum and energy are used. In the mentioned studies, it was assumed that the enhancement of the convective heat transfer is just because of the enhancement in the thermal conductivity, and the only effect of nanoparticles is the effect on the thermo-physical properties of the base fluid. In the homogenous models, the nanoparticles are in thermal equilibrium with the base fluid and there are no slip velocities between the nanoparticles and fluid molecules. Thus, a uniform mixture of nanoparticles is considered for the nanofluid. From this point of view some researchers analyzed the natural convection of nanofluids. Khanafer *et al*. (2003) studied the natural convection of Cu-water nanofluids in a two-dimensional enclosure and found that an increase of the nanoparticle volume fraction increased the Nusselt number. Following this work Jou and Tzeng (2006) repeated the proposed problem with different aspect ratios of the enclosure, and the same results were obtained. Noghrehabadi *et al*. (2012a) studied the forced convection heat transfer of Ag-water and SiO_2 nanofluids over a stretching sheet. Hady *et al*. (2011) analyzed natural convection of water-based nanofluids over a full cone embedded in a porous medium. They found that the local Nusselt number decreased with an increase of the nanoparticle volume fraction for copper (Cu), silver (Ag), alumina (Al_2O_3) and titanium oxide (TiO_2) nanoparticles.

From another point of view, it is believed that, in the convection of nanofluids, there are several slip mechanisms, so the volume fraction of nanoparticles in the nanofluid may not be uniform. The consideration of additional heat transfer mechanisms in the convective heat transfer problems was taken one step further by Buongiorno (2006). Buongiorno discussed seven possible mechanisms: inertia, Brownian diffusion, thermophoresis, diffusionphoresis, the Magnus effect, fluid drainage, and gravity for particle slip during the convection of nanofluids, of which thermophoresis and the Brownian diffusion were found to be important.

Only a few studies have been performed of convection with models including slip mechanisms. Noghrehabadi *et al*. (2012b; 2012c; 2013a; 2013b) analyzed different aspects of the boundary layer heat transfer of nanofluids over a stretching sheet. Kuznetsov and Nield (2010; 2011) examined natural convective boundary-layer flow of a nanofluid past a vertical plate, and they found that the reduced Nusselt number is a decreasing function of Brownian motion and the thermophoresis parameter. Khan and Aziz (2011) studied natural convection of nanofluids over a vertical flat plate with uniform surface heat flux. They found that for a fixed Lewis number, the reduced Nusselt number is a decreasing function of the Brownian motion parameter, the thermophoresis parameter and the buoyancy ratio parameter.

In the area of heat transfer of nanofluids including slip mechanisms in porous media very few researches have been done. Nield and Kuznetsov (2009) studied the classical Cheng–Minkowycz problem for natural convective boundary-layer flow in a porous medium saturated by a nanofluid. Chamkha *et al.* (2011) presented a non-similar solution for natural convective boundary layer flow over a sphere embedded in a porous medium saturated with a nanofluid. Rashad *et al*. (2011) investigated the natural convection

boundary layer of a nanofluid about a permeable vertical full cone embedded in a saturated porous medium. The non-Darcy effects of porous medium on the boundary layer heat transfer of nanofluids over a cone have been examined by Noghrehabadi *et al*. (2013c). Natural convective boundary layer flow over a horizontal plate embedded in a porous medium saturated with a nanofluid has been investigated by Gorla and Chamkha (2011). Mixed convective boundary layer flow over a vertical wedge embedded in a porous medium saturated with a nanofluid has been analyzed by Gorla *et al.* (2011). Noghrehabadi *et al*. (2013d) have examined the natural convection boundary layer flow of a nanofluid over a vertical plate with surface heat flux embedded in a saturated porous medium.

Aziz and Khan (2011) have studied the natural convective flow of a nanofluid over a convectively heated vertical plate in a clear, non-porous space. They found that an increase of the convective heating parameter increased the dimensionless temperature and dimensionless velocity profiles. They reported that an increase of the Brownian motion and thermophoresis parameters increases the dimensionless temperature profiles but decreases the concentration profiles.

To the best of authors' knowledge, there is no investigation that addressed the effect of the convective heating condition on the heat transfer characteristics of natural convection of nanofluids over a vertical flat plate in a porous medium with a model which incorporates the Brownian motion and thermophoresis effects of nanoparticles. The present study examines the effect of parametric variation of the Brownian motion and thermophoresis as important parameters in natural convection of nanofluids over a convectively heated vertical plate embedded in a porous medium on the boundary layer flow, heat and mass transfer of nanofluids.

MATHEMATICAL FORMULATION

Consider the two-dimensional and steady natural convection boundary layer flow of a nanofluid past a convectively heated vertical plate which is placed in a porous medium saturated with a nanofluid. The coordinate system is chosen such that the x-axis is aligned with the flow over the plate. The scheme of the physical model and the coordinate system is shown in Fig. 1.

It is worth mentioning that there are three distinct boundary layers, namely the hydrodynamic boundary layer, thermal boundary layer, and nanoparticle concentration boundary layer, but only one boundary layer is shown in this figure to avoid congestion. It is assumed that the nanoparticle volume fraction (φ) at the wall surface ($y = 0$) takes the constant value of φ_w.

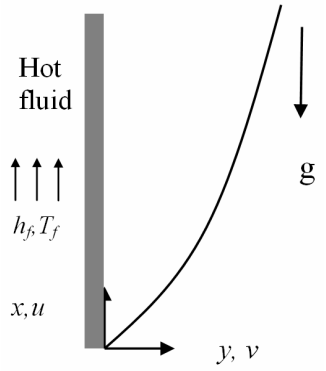

Figure 1: The physical model and the coordinate systems utilized to model convective heat transfer past a vertical plate embedded inside a homogeneous porous media saturated with a nanofluid.

The ambient values of T and φ are denoted by T_∞ and φ_∞, respectively. The flow in porous media with porosity of ε and permeability of κ is considered as the Darcy flow. It is assumed that the porous medium is homogeneous, and the porous medium and nanofluid are in local thermal equilibrium. By employing the Oberbeck-Boussinesq approximation and applying the standard boundary layer approximations, the basic steady conservation of total mass, momentum, thermal energy, and nanoparticles for the nanofluids can be written in the Cartesian coordinate system of x and y as follows (Nield and Kuznetsov, 2009),

$$\frac{\partial u}{\partial x}+\frac{\partial v}{\partial y}=0. \tag{1}$$

$$\frac{\partial p}{\partial y}=0. \tag{2a}$$

$$\frac{\mu}{\kappa}u=\begin{bmatrix}-\left(\dfrac{\partial p}{\partial x}-(1-\phi_\infty)\beta g\rho_{f_\infty}\left(T-T_\infty\right)\right)\\ -\left(\rho_P-\rho_{f_\infty}\right)g\left(\phi-\phi_\infty\right)\end{bmatrix}. \tag{2b}$$

$$u\frac{\partial T}{\partial x}+v\frac{\partial T}{\partial y}=\alpha_m\nabla^2 T +\tau\left[D_B\frac{\partial \varphi}{\partial y}\frac{\partial T}{\partial y}+\frac{D_T}{T_\infty}\left(\frac{\partial T}{\partial y}\right)^2\right]. \tag{3}$$

$$\frac{1}{\varepsilon}\left[u\frac{\partial \phi}{\partial x}+v\frac{\partial \phi}{\partial y}\right]=D_B\frac{\partial^2 \phi}{\partial y^2}+\left(\frac{D_T}{T_\infty}\right)\frac{\partial^2 T}{\partial y^2}. \quad (4)$$

subject to the following boundary conditions,

$$v=0,\quad -k\frac{\partial T}{\partial y}=h_f(T_f-T),\quad \phi=\phi_W,\quad at\quad y=0. \quad (5)$$

$$u\to u_\infty,\ T\to T_\infty,\quad \phi\to\phi_\infty,\quad at\quad y\to\infty. \quad (6)$$

where

$$\alpha_m=\frac{k_m}{(\rho c)_f},\qquad \tau=\frac{\varepsilon(\rho c)_p}{(\rho c)_f}. \quad (7)$$

The pressure can be eliminated from Eqs. (2a) and (2b) by cross-differentiation. Introducing the following stream function (ψ), the continuity equation is automatically satisfied.

$$u=\frac{\partial \psi}{\partial y},\qquad v=-\frac{\partial \psi}{\partial x}, \quad (8)$$

Here the local Rayleigh number Ra_x can be introduced as (Gorla *et al*., 2011):

$$Ra_x=\frac{(1-\phi_\infty)\rho_{f\infty}\beta g\kappa x(T_f-T_\infty)}{\mu\alpha_m}, \quad (9)$$

where η is the similarity variable:

$$\eta=\frac{y}{x}Ra_x^{\frac{1}{2}} \quad (10)$$

The dimensionless similarity variables, S, η, and f are introduced as follows:

$$S=\frac{\psi}{\alpha_m Ra_x^{\frac{1}{2}}},\quad f=\frac{\phi-\phi_\infty}{\phi_w-\phi_\infty},\quad \theta=\frac{T-T_\infty}{T_f-T_\infty}. \quad (11)$$

After applying Eqs. (10) and (11) in Eqs. (1)-(4), the following three ordinary differential equations are obtained (See Appendix),

$$S''-\theta'+Nr.f'=0. \quad (12)$$

$$\theta''+\frac{1}{2}.S\theta'+Nb.f'.\theta'+Nt(\theta')^2=0. \quad (13)$$

$$f''+\frac{1}{2}.Le.S.f'+\frac{Nt}{Nb}\theta''=0. \quad (14)$$

subject to the following boundary conditions:

$$\eta=0:\quad S=0,\quad \theta'(0)=-Nc(1-\theta(0)),\quad f=1. \quad (15)$$

$$\eta\to\infty:\ S'=0,\quad \theta=0,\quad f=0. \quad (16)$$

where

$$Nr=\frac{(\rho_p-\rho_{f\infty})(\phi_w-\phi_\infty)}{\rho_{f\infty}\beta(T_w-T_\infty)(1-\phi_\infty)}, \quad (17a)$$

$$Nb=\frac{\varepsilon(\rho c)_p D_B(\phi_w-\phi_\infty)}{(\rho c)_f\alpha_m}, \quad (17b)$$

$$Nt=\frac{\varepsilon(\rho c)_p D_T(T_w-T_\infty)}{(\rho c)_f\alpha_m T_\infty}, \quad (17c)$$

$$Le=\frac{\alpha_m}{\varepsilon D_B}, \quad (17d)$$

$$Nc=\frac{h_f x^{\frac{1}{2}}}{k\left(\frac{(1-\phi_\infty)\beta\kappa g(T_f-T_\infty)}{\mu\alpha}\right)^{\frac{1}{2}}} \quad (17e)$$

where Nr is the buoyancy-ratio parmeter, Nb is the Brownian motion parameter, Nt is the thermophoresis parameter, Le is the Lewis number, and Nc is the convective heating parameter. In Equation (17e) the convective heating parameter (Nc) depends on x. However, if the convective heat transfer coefficient (h_f) is proportional to $x^{-1/2}$, Nc becomes independent of x and a true similarity is realized. For Nc→∞, the convective boundary condition reduces to the constant surface temperature boundary condition analyzed by Nield and Kuznetsov (2009). It is worth mentioning that the convective parameter (Nc) is related to the traditional Biot number and the Rayleigh number as $Nc=Bi_x/Ra_x^{1/2}$ where $Bi_x=h_f x/k$.

The quantities of local Nusselt number (Nu_x) and local Sherwood number (Sh_x) can be introduced as:

$$Nu_x = \frac{q_W x}{k\left(T_W - T_\infty\right)}. \tag{18}$$

$$Sh_x = \frac{q_m x}{D_B\left(\phi_W - \phi_\infty\right)}. \tag{19}$$

where the quantity q_w is the wall heat flux because of the temperature gradient and q_m is the wall mass flux because of the Brownian motion force. Using similarity transforms introduced in Eq. (11), the reduced Nusselt number (*Nur*) and reduced Sherwood number (*Shr*), as important parameters in heat and mass transfer, can be obtained as,

$$Ra_x^{-\frac{1}{2}} Nu_x = -\theta'(0). \tag{20}$$

$$Ra_x^{-\frac{1}{2}} Sh_x = -f'(0). \tag{21}$$

NUMERICAL METHOD

Consider the system of Eqs. (12)-(14) subject to the boundary conditions of Eqs. (15)-(16). The system of equations is numerically solved using the iterative fourth-order Runge-Kutta method associated with the Gauss-Newton method (Dennis, 1977) starting with an initial guess. In this method, every n*th*-order equation is converted to *n* first order equations. Therefore, the system of ordinary differential equations is converted into a system of first-order equations. An iteration method is then applied on the latter system to adjust the initial guess using the Gauss-Newton method. The η direction is divided into 300 nodal points so that the results become accurate. The Gauss-Newton approach is utilized to update the initial guesses until the asymptotic boundary conditions are reached. A maximum relative error of 10^{-5} is used as the stopping criteria for the iterations. The most crucial factor of this numerical solution is to choose the appropriate finite value of η_∞. Thus, the asymptotic boundary conditions given by Eq. (16) were replaced by using a comparatively large value of η_{max}=10. The choice of η_{max}=10 ensured that all numerical solutions approached the asymptotic values correctly.

As a test of the accuracy of the solution, the value of *Nur* is compared with the value reported by Cheng and Minkowycz (1977) in Table 1 when the effects of nanofluid parameters are neglected.

Table 1: Comparison of results for the reduced Nusselt number -θ'(0).

Cheng and Minkowycz (1977)	Present result
0.4440	0.4439

RESULTS AND DISCUSSION

In the present study, the values of the convective heating parameter (*Nc*) are chosen as less than unity (*Nc*=0.2), higher than unity (*Nc*=2) and very high (*Nc*=1000) to obviously show the effect of different values of this parameter on the dimensionless velocity, temperature and concentration profiles as well as reduced Nusselt number and reduced Sherwood number. The increase of the convective heating parameter from very low to very high values demonstrates that the value of *Nc*=1000 can accurately simulate the isothermal boundary condition, which has been previously considered by Nield and Kuznetsov (2009). Therefore, *Nc*=1000 is considered as the physical infinity in the following text. It is noted that, in the case of *Nc*=1000, the wall temperature is very close to the hot fluid temperature T_f.

Since most nanofluids examined to date have large values of the Lewis number *Le* > 1 (Nield and Kuznetsov, 2009), the values of *Le*=10 and *Le*=100 have been examined in the present study. The choice of values for *Nr*, *Nb* and *Nt* was dictated by the fact that these values were used by Nield and Kuznetsov (2009) for the isothermal wall case. By using the same values of *Nr*, *Nb* and *Nt,* the present work on the convective boundary condition can be viewed in proper perspective with the isothermal results.

The values of reduced Nusselt number ($-\theta'(0)$) and reduced Sherwood number ($-f'(0)$) are shown in Table 2 and Table 3, respectively, for selected combinations of *Nt*, *Nb* and *Nr* and two selected values of Lewis number and the fixed value of convective heating parameter (*Nc*=10). The results of Table 2 depict that an increase of the Brownian motion parameter as well as the buoyancy ratio parameter decreases the reduced Nusselt number; an increase of thermophoresis parameter also decreases the reduced Nusselt number.

The trend of results reported by Aziz and Khan (2011) in tabular form reveals that an increase of *Nb* and *Nr* decreases the reduced Nusselt number. The trend of the results of Aziz and Khan (2011) is in agreement with the results of the present study.

From Table 2, it is realized that the increase of the Lewis number for a low value of *Nr* (i.e., *Nr*=0.1) decreases the reduced Nusselt number; whereas for a high value of *Nr* (i.e., *Nr*=0.5), the increase of the Lewis number increases the values of the reduced Nusselt number.

The trend of results presented by Aziz and Khan (2011) in tabular form for the values of *Nb*>0.3 is similar to the results of the present study. The work of Aziz and Khan (2011) shows that the increase of the Lewis number decreases the reduced Nusselt number for low values of *Nr,* whereas the increase of Lewis number increases the reduced Nusselt number for high values of *Nr*.

The results of Table 3 show that the reduced Sherwood number is an increasing function of the Brownian motion parameter (*Nb*), but is a decreasing function of the bouancy ratio parameter (*Nr*). As seen, an increase of the thermophoresis parameter (*Nt*) increases the reduced Sherwood number for the high value of Lewis number (i.e., *Le*=100), whereas the reduced Sherwood number is decreased by an increase of *Nt* for the small values of *Le* and *Nb* (i.e., *Le*=10, *Nb*<0.3). In addition, an increase of *Nt* increases the reduced Sherwood number for the large value of *Nb* (i.e., *Nb*=0.5) and the small value of *Le* (i.e., *Le*=10). The reduced Sherwood number is increased by an increase of the Lewis number.

Table 2: The effect of the Brownian motion parameter, thermophoresis parameter, buoyancy ratio parameter and Lewis number on the reduced Nusselt number (-θ '(0)) when *Nc*=10.

-θ'(0)							
Nb	***Nt***	**Nr=0.1**		**Nr=0.3**		**Nr=0.5**	
		Le=10	**Le=100**	**Le=10**	**Le=100**	**Le=10**	**Le=100**
0.1	**0.1**	0.36469	0.36445	0.34613	0.35854	0.32525	0.35180
	0.2	0.35107	0.35066	0.33135	0.34477	0.30937	0.33808
	0.3	0.33811	0.33753	0.31749	0.33168	0.29463	0.32509
	0.4	0.32579	0.32504	0.30448	0.31926	0.28095	0.31277
	0.5	0.31408	0.31316	0.29226	0.30746	0.26824	0.30110
0.3	**0.1**	0.31429	0.30527	0.30015	0.30070	0.28423	0.29549
	0.2	0.30287	0.29360	0.28882	0.28916	0.27308	0.28412
	0.3	0.29197	0.28249	0.27806	0.27819	0.26255	0.27332
	0.4	0.28156	0.27194	0.26784	0.26777	0.25260	0.26306
	0.5	0.27163	0.26190	0.25812	0.25786	0.24318	0.25331
0.5	**0.1**	0.26929	0.25495	0.25783	0.25132	0.24495	0.24720
	0.2	0.25942	0.24508	0.24820	0.24158	0.23564	0.23761
	0.3	0.25001	0.23570	0.23904	0.23232	0.22681	0.22850
	0.4	0.24102	0.22679	0.23032	0.22353	0.21843	0.21986
	0.5	0.23245	0.21832	0.22203	0.21519	0.21047	0.21165

Table 3: The effect of the Brownian motion parameter, thermophoresis parameter, buoyancy ratio parameter and Lewis number on the reduced Sherwood number (-*f* '(0)) when *Nc*=10.

-f'(0)							
Nb	***Nt***	**Nr=0.1**		**Nr=0.3**		**Nr=0.5**	
		Le=10	**Le=100**	**Le=10**	**Le=100**	**Le=10**	**Le=100**
0.1	**0.1**	1.50046	5.24280	1.37230	4.83916	1.22911	4.39348
	0.2	1.42705	5.24059	1.30457	4.83946	1.16789	4.39680
	0.3	1.36794	5.24514	1.25041	4.84641	1.11946	4.40672
	0.4	1.32170	5.25545	1.20816	4.85900	1.08193	4.42212
	0.5	1.28700	5.27065	1.17638	4.87633	1.05366	4.44211
0.3	**0.1**	1.59056	5.29650	1.45939	4.89417	1.31335	4.45068
	0.2	1.58107	5.31251	1.45166	4.91139	1.30772	4.46949
	0.3	1.57535	5.32958	1.44754	4.92960	1.30553	4.48918
	0.4	1.57300	5.34743	1.44661	4.94854	1.30636	4.50953
	0.5	1.57365	5.36585	1.44852	4.96799	1.30985	4.53033
0.5	**0.1**	1.61724	5.32408	1.48642	4.92372	1.34110	4.48294
	0.2	1.61917	5.34170	1.48934	4.94221	1.34526	4.50264
	0.3	1.62280	5.35933	1.49390	4.96068	1.35098	4.52221
	0.4	1.62794	5.37686	1.49989	4.97900	1.35805	4.54159
	0.5	1.63441	5.39421	1.50712	4.99711	1.36628	4.56070

When the parameters of the nanofluid are taken to be zero (i.e. *Nr*=*Nb*=*Nt*=0), the nanofluid model is reduced to the pure fluid model. In the case of the isothermal boundary condition (i.e., *Nc*=1000) and pure fluid, the results show that the velocity and temperature profiles are identical. These findings are in good agreement with those reported by Cheng and Minkowycz (1977) who studied free convection about an isothermal vertical plate embedded in a porous medium. The velocity and temperature profiles of a pure fluid for selected values of the convective heating parameter are plotted in Fig. 2. This figure shows that the temperature and velocity profiles are identical in the case of pure fluid and for all values of convective heating parameter. It is clear that, in the case of a pure fluid, the increase of *Nc* increases the dimensionless velocity and temperature profiles.

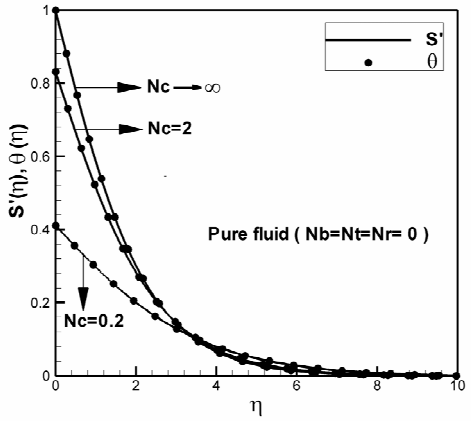

Figure 2: The temperature and velocity boundary layer profiles obtained in the present study in the case of pure fluid for various values of the convection heating parameter (*Nc*).

The non-dimensional profiles of velocity, temperature and concentration are plotted in Fig. 3 when *Nt*=*Nb*=*Nr*=0.5, *Le*=10 and *Nc*=2. This figure reveals that the dimensionless thermal and velocity boundary layers are of comparable thickness. However, they are not identical. The nanoparticle concentration boundary layer is much thinner than the thermal and the velocity boundary layers.

The comparison between the dimensionless velocity profiles in two cases of pure fluid (Fig. 2) and nanofluid (Fig. 3) is interesting. It shows that these profiles in the case of a pure fluid are decreased asymptotically to zero at the edge of the hydrodynamic boundary layer, but in the case of the nanofluid first they increase to a maximum velocity and then decrease asymptotically to zero at the edge of the hydrodynamic boundary layer. This observed difference is because of the presence of the slip mechanisms between nanoparticles and the base fluid.

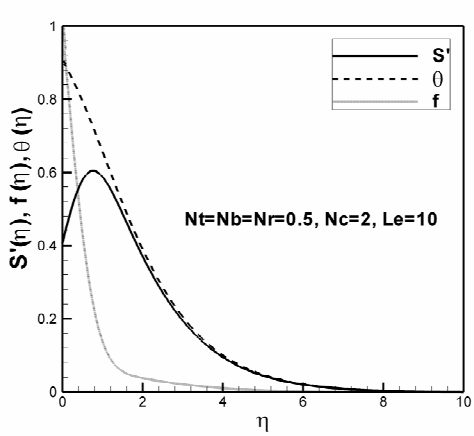

Figure 3: The temperature, velocity and concentration boundary layer profiles of a nanofluid when *Nt*=*Nb*=*Nr*=0.5, *Nc*=2 and *Le*=10.

The thermophoresis parameter (*Nt*) can be described as the ratio of the nanoparticle diffusion due to the thermophoresis force to the thermal diffusion in the nanofluid. Buongiorno reported that the solid nanoparticles in the nanofluid experience a force in the direction opposite to the imposed temperature gradient. Hence, the nanoparticles tend to move from hot to cold.

The non-dimensional profiles of the nanoparticle volume fraction, temperature and velocity are shown in Figs. 4-6, respectively, for different values of thermophoresis and convective heating parameters when the buoyancy-ratio parameter (*Nr*), Brownian motion parameter (*Nb*) and Lewis number (*Le*) are kept fixed. These figures indicate that an increase of *Nt* increases the magnitude of the velocity, temperature and concentration profiles. The atoms which are near the hot wall carry more momentum than those atoms which are far from the wall (in colder regions). The different momenta which a solid particle receives from hot and cold fluid atoms (because of the temperature gradient) result in a force which is known as the thermophoresis force (Zheng, 2002). An increase of *Nc* increases the magnitude of the velocity and temperature profiles, but decreases the magnitude of the concentration profiles. Therefore, it is expected that the increase of *Nt* increases the force on the nanoparticles in the direction away from the hot wall and increases the diffusion of nanoparticles into the nanofluid, which is shown in Fig. 4. Consequently, an increase of *Nt* increases the non-dimensional temperature at the wall, which is clearly shown in Fig. 5. An increase of the thermophoresis

force increases the movement of nanoparticles and consequently increases the non-dimensional velocity profiles, which is depicted in Fig. 6.

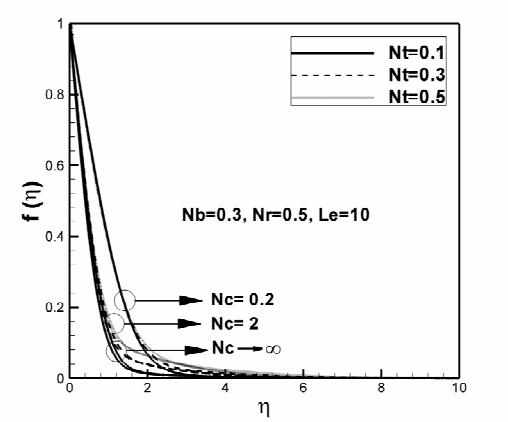

Figure 4: The boundary layer nanoparticle concentration profiles for selected values of the thermophoresis parameter (*Nt*) and convection heating parameter (*Nc*).

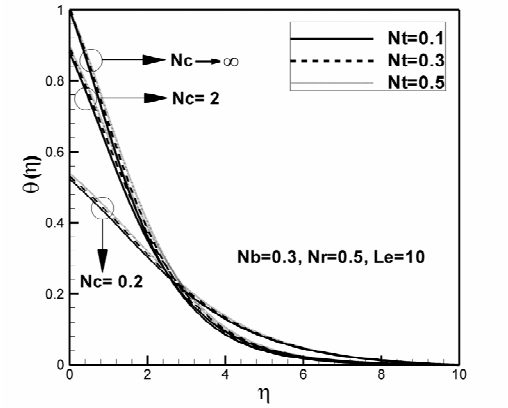

Figure 5: The boundary layer temperature profiles for selected values of the thermophoresis parameter (*Nt*) and convection heating parameter (*Nc*).

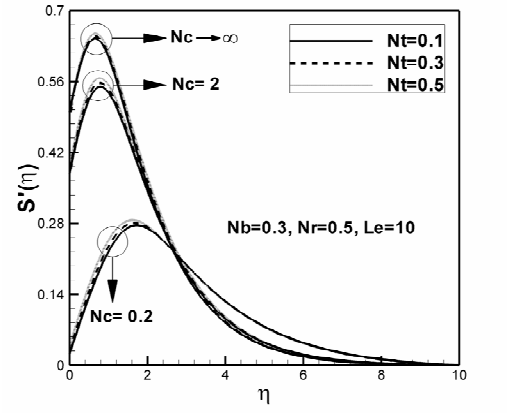

Figure 6: The boundary layer velocity profiles for selected values of the thermophoresis parameter (*Nt*) and convection heating parameter (*Nc*).

The thermophoresis parameter is independent of the particle diameter in the case of very small particles (Buongiorno, 2006). For comparatively low values of *Nc* the profiles of velocity, temperature and concentration are significantly influenced by variation of the convective heating parameter (*Nc*). The increase of *Nc* increases the concentration profiles in the boundary layer. The increase of the convective heating parameter increases the non-dimensional temperature and velocity profiles near the wall, but near the edge of the boundary layer the increment of *Nc* slightly decreases the temperature and velocity profiles.

The Brownian motion parameter can be described as the ratio of the nanoparticle diffusion due to the Brownian motion effect to the thermal diffusion in the nanofluid. Based on the Einstein-Stokes equation (Buongiorno, 2006), the Brownian motion is proportional to the inverse of the particle diameter (Buongiorno, 2006). Hence, as the particle diameter decreases, the Brownian motion increases. Figs. 7-9 show the variation of the non-dimensional profiles for different values of the Brownian motion parameter and selected values of the convective heating parameter. It is observed that, with an increase of the Brownian motion parameter, the magnitude of the velocity and temperature profiles increases, but the magnitude of the concentration profiles decreases. These findings are similar to the results reported by Aziz and Khan (2011). They reported that an increase of the Brownian motion parameter increases the temperature profiles and decreases the concentration profiles. Increase of the Brownian motion parameter increases the diffusion of particles, which results in the increase of the magnitude of the temperature profiles (Fig. 8).

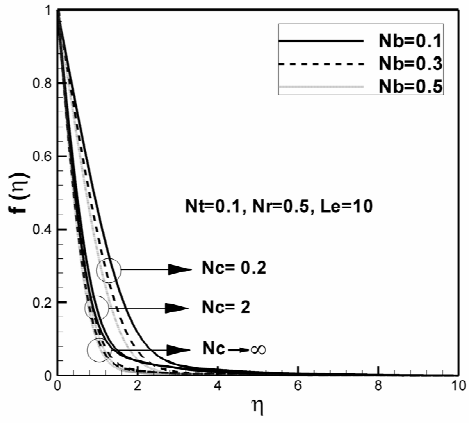

Figure 7: The boundary layer nanoparticle concentration profiles for selected values of the Brownian motion parameter (*Nb*) and convection heating parameter (*Nc*).

It is interesting that the variation of the convective heating parameter, Brownian motion or thermophoresis parameter does not have a significant effect on the thickness of the hydrodynamic, thermal and concentration boundary layers. Comparison between Figs. 5 and 6, as well as comparison between Figs. 8 and 9, shows that the temperature and velocity profiles are not identical, even in the case of high values of the convective heating parameter (i.e., isothermal surface). As was mentioned before, this is because of the presence of slip mechanisms of nanoparticles which affect the thermal and hydrodynamic boundary layers.

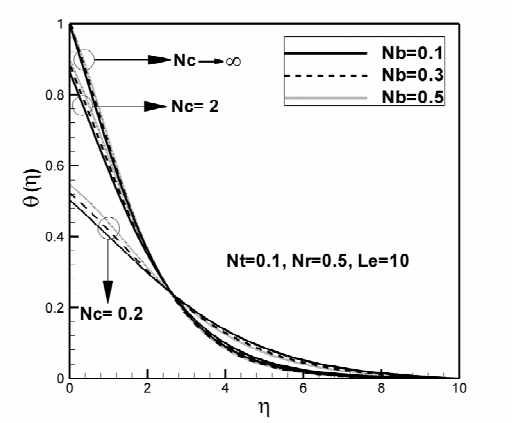

Figure 8: The boundary layer temperature profiles for selected values of the Brownian motion parameter (*Nb*) and convection heating parameter (*Nc*).

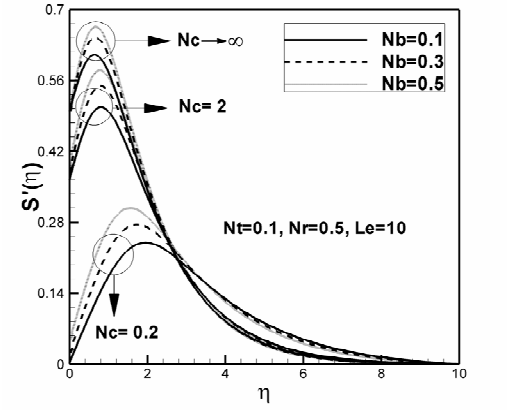

Figure 9: The boundary layer velocity profiles for selected values of the Brownian motion parameter (*Nb*) and convection heating parameter (*Nc*).

The variation of the dimensionless heat transfer rate parameter (reduced Nusselt number), mass transfer rate (reduced Sherwood number) and surface temperature as a function of the thermophoresis parameter are shown in Figs. 10, 11 and 12, respectively, for *Nr*=0.5 and *Le*=10 and for selected values of the convective heating parameter. Figs. 10 and 11 show that the increase of *Nb* decreases the dimensionless heat transfer rate but increases the dimensionless mass transfer rate. Furthermore, the increase of *Nt* decreases the reduced Nusselt number and reduced Sherwood number. Increase of the Brownian motion parameter increases the diffusion of nanoparticles due to the Brownian effect and consequently decreases the reduced Nusselt number (-θ'(0)), as observed in Figure 10.

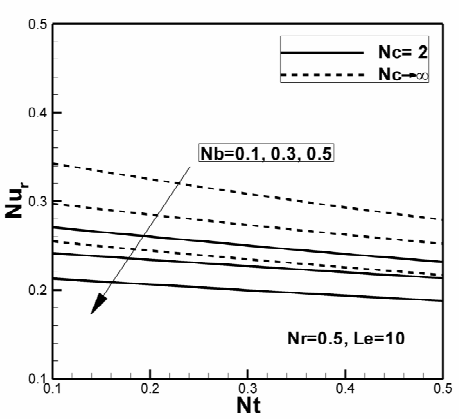

Figure 10: The reduced Nusselt number (*Nur*) as a function of the thermophoresis parameter for selected values of the Brownian motion parameter (*Nb*) and convection heating parameter (*Nc*).

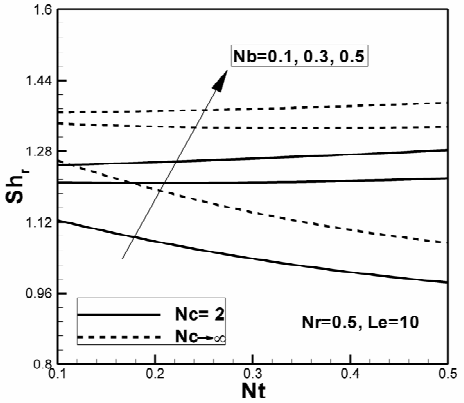

Figure 11: The reduced Sherwood number (*Nur*) as a function of the thermophoresis parameter for selected values of the Brownian motion parameter (*Nb*) and convection heating parameter (*Nc*).

Figure 11 shows that, for comparatively small values of *Nb* (i.e., *Nb*=0.1), the variation of *Nt* has a significant effect on the variation of reduced Sherwood number, but with the increase of *Nb* this effect is reduced. An increase of nanoparticle diffusion due to the increase of the Brownian motion parameter increases the nanoparticle concentration in the vicinity of the wall surface and, consequently, it increases the reduced Sherwood number (-*f* '(0)).

Finally, an increase of the convective heating parameter increases the reduced Nusselt and Sherwood numbers. The trend of the results reported by Aziz and Khan (2011) is similar to the present results. They found that an increase of the convective heating parameter increased the reduced Nusselt number. This is reasonable because stronger convective heating on the back side of the plate must result in higher heat dissipation to the nanofluid on the front of the plate.

Nield and Kuznetsov (2009) reported that an increase in the buoyancy-ratio number, the Brownian motion parameter or the thermophoresis parameter leads to a decrease in the value of the reduced Nusselt number (corresponding to an increase in the thermal boundary-layer thickness), which is in full agreement with the present findings.

Fig. 12 reveals that an increase of the convective heating parameter tends to change the thermal boundary condition from a convective heating boundary condition to the isothermal boundary condition. An increase of *Nb* increases the motion of nanoparticles due to the Brownian effect, which results in the increase of the diffusion of nanoparticles into the fluid and leads to an increase of the non-dimensional surface temperature.

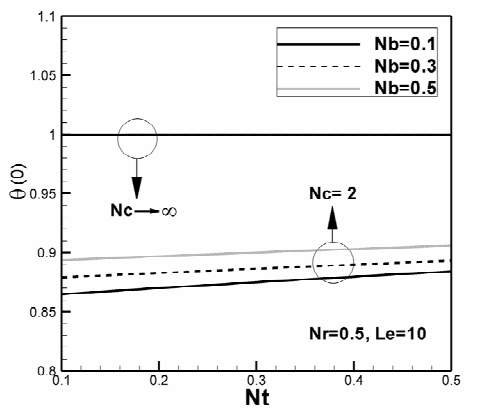

Figure 12: The non-dimensional wall temperature as a function of the thermophoresis parameter (*Nt*) for selected values of the Brownian motion parameter (*Nb*) and convection heating parameter (*Nc*).

CONCLUSIONS

In the present work, a combined similarity and numerical approach has been used to investigate the natural convection over a convectively heated vertical plate embedded in a porous medium saturated with a nanofluid. In the modeling of the nanofluid, the dynamic effects of nanoparticles, thermophoresis and Brownian motion have been taken into account. The natural convection boundary layer depends on five dimensionless parameters, namely the thermophoresis parameter *Nt*, Brownian motion parameter *Nb*, Lewis number *Le*, buoyancy ratio parameter *Nr* and convective heating parameter *Nc*. The findings of the present study can be summarized as follows:

The temperature and velocity profiles for the nanofluids are of comparable thickness, but the thickness of the concentration profiles is much lower than those of temperature and velocity profiles.

The velocity, temperature and concentration profiles are an increasing function of the thermophoresis parameter (*Nt*). However, the effect of the thermophoresis parameter on the concentration profiles in the vicinity of the wall in not significant.

As the Brownian motion parameter increases, the velocity and temperature profiles increase. However, the concentration profiles are a decreasing function of the Brownian motion parameter. It is interesting that the variation of the Brownian motion parameter does not show a significant influence on the concentration and temperature profiles, but its effect on the velocity profiles is obvious in the vicinity of the wall.

As the convective heating parameter (*Nc*) increases, the velocity and temperature profiles rise in the vicinity of the wall. However, this effect is inverted far from the wall. The concentration profiles are a decreasing function of the convective heating parameter (*Nc*) in the entire boundary layer.

When the values of *Le* and *Nr* are kept constant, an increase of Brownian motion increases the reduced Sherwood number and decreases the reduced Nusselt number.

For low values of the convective heating parameter, as the Brownian motion parameter increases, the non-dimensional wall temperature increases. However, for high values of *Nc*, the effect of the Brownian motion parameter on the non-dimensional wall temperature is not significant.

Both the reduced Nusselt and Sherwood numbers are an increasing function of the convective heating parameter.

Currently, there are few concrete experimental reports on the coefficients of thermophoresis and Brownian motion for nanoparticles in fluids. Therefore, the exact ranges of the Lewis number, Brownian motion parameter and the thermophoresis parameter have not been discussed in detail. The range of these parameters was selected based on the range of these parameters in previous studies. Hence, future experimental or analytic studies are strongly demanded in this area. In addition, the concentration

of the nanoparticles on the wall was assumed to be constant. This is an over simplified boundary condition for the nanofluid and nanoparticles. Introducing more realistic experimental or analytical boundary conditions for the concentration of nanoparticles at the wall is crucial.

ACKNOWLEDGEMENTS

The authors are grateful to Shahid Chamran University of Ahvaz for its crucial support. The authors would also thank Ali Behseresht for his assistant in some parts of the paper.

NOMENCLATURE

(x, y)	Cartesian coordinates
Nc	Convective heating parameter
D_B	Brownian diffusion coefficient
D_T	thermophoretic diffusion coefficient
f	rescaled nanoparticle volume fraction, nanoparticle concentration
g	gravitational acceleration vector
κ	permeability of the porous medium
k	thermal conductivity
k_m	effective thermal conductivity of the porous medium and nanofluid
Le	Lewis number
Nb	Brownian motion parameter
Nr	buoyancy ratio
Nt	thermophoresis parameter
P	pressure
Ra_x	local Rayleigh number
S	dimensionless stream function
T	temperature
T_∞	ambient temperature
T_W	wall temperature of the vertical plate
U	reference velocity
u, v	Darcy velocity components

Greek Symbols

$(\rho c)_f$	heat capacity of the nanofluid
$(\rho c)_m$	effective heat capacity of the porous medium
$(\rho c)_p$	effective heat capacity of the nanoparticle material
μ	viscosity of the nanofluid
α_m	effective thermal diffusivity of the porous medium and nanofluid
β	volumetric expansion coefficient of the fluid
ε	porosity
η	dimensionless distance
θ	dimensionless temperature
ρ_f	fluid density
ρ_p	nanoparticle mass density
τ	parameter defined by Eq. (7)
φ	nanoparticle volume fraction
φ_∞	ambient nanoparticle volume fraction
φ_w	nanoparticle volume fraction at the wall of the vertical plate
ψ	stream function

REFERENCES

Aziz, A., Khan, W. A., Natural convective boundary layer flow of a nanofluid past a convectively heated vertical plate. International Journal of Thermal Sciences, 52, 83-90 (2012).

Buongiorno, J., Convective transport in nanofluids. J. Heat Transfer, 128, 240-250 (2006).

Chamkha, A., Gorla, R. S. R., Ghodeswar, K., Non-similar solution for natural convective boundary layer flow over a sphere embedded in a porous medium saturated with a nanofluid. Transp Porous Med., 86, 13-22 (2011).

Chang, B. H., Mill, A. F., Hernandez, E., Natural convection of microparticle suspensions in thin enclosures. International Journal of Heat and Mass Transfer, 51, 1332-1341 (2008).

Cheng, P., Minkowycz, W. J., Free convection about a vertical flat plate embedded in a saturated porous medium with applications to heat transfer from a dike. J. Geophysics. Res., 82, 2040-2044 (1977).

Das, S. K., Choi, S. U. S., Yu, W., Pradeep, T., Nanofluids: Science and Technology, Hoboken: John Wiley & Sons (2007).

Daungthongsuk, W., Wongwises, S., A critical review of convective heat transfer of nanofluids. Renewable and Sustainable Energy Reviews, 11(5), 797-817 (2007).

Dennis, J. E., Nonlinear Least-Squares, State of the Art in Numerical Analysis. Ed. D. Jacobs, Academic Press: 269-312 (1977).

Gorla, R. S. R., Chamkha, A., Natural convective boundary layer flow over a horizontal plate embedded in a porous medium saturated with a

nanofluid. Journal of Modern Physics, 2, 62-71 (2011).

Gorla, R. S. R., Zinolabedini free convection from a vertical plate with nonuniform surface temperature and embedded in a porous medium. Transactions of Journal of Energy Resources Technology, 109, 26-30 (1987).

Gorla, R. S. R., Chamkha, A. J., Rashad, A. M., Mixed convective boundary layer flow over a vertical wedge embedded in a porous medium saturated with a nanofluid- Natural Convection Dominated Regime. Nanoscale Research Letters, 6, 1-9 (2011).

Hady, F. M., Ibrahim, F. S., Abdel-Gaied, S. M., Eid, M. R., Effect of heat generation/absorption on natural convective boundary-layer flow from a vertical cone embedded in a porous medium filled with a non-Newtonian nanofluid. International Communications in Heat and Mass Transfer, 38, 1414-1420 (2011).

Hamad, M. A. A., Analytical solution of natural convection flow of a nanofluid over a linearly stretching sheet in the presence of magnetic field. International Communications in Heat and Mass Transfer, 38, 487-492 (2011).

Hwang, K. S., Jang, S. P., Choi, S. U. S., Flow and convective heat transfer characteristics of water-based Al_2O_3 nanofluids in fully developed laminar flow regime. International Journal of Heat and Mass Transfer, 52, 193-199 (2009).

Jou, R. Y., Tzeng, S. C., Numerical research of nature convective heat transfer enhancement filled with nanofluids in rectangular enclosures. International Communications in Heat and Mass Transfer, 33, 727-736 (2006).

Kakaç, S., Pramuanjaroenkij, A., Review of convective heat transfer enhancement with nanofluids. International Journal of Heat and Mass Transfer, 52, 3187-3196 (2009).

Khan, W. A., Aziz, A., Natural convection flow of a nanofluid over a vertical plate with uniform surface heat flux. International Journal of Thermal Sciences, 50, 1207-1214 (2011).

Khanafer, K., Vafai, K., Lightstone, M., Buoyancy-driven heat transfer enhancement in a two-dimensional enclosure utilizing nanofluids. Int. J. Heat Mass Transfer, 46, 3639-3653 (2003).

Kuznetsov, A. V., Nield, D. A., Natural convective boundary-layer flow of a nanofluid past a vertical plate. International Journal of Thermal Sciences, 49, 243-247 (2010).

Kuznetsov, A. V., Nield, D. A., Double-diffusive natural convective boundary-layer flow of a nanofluid past a vertical plate. International Journal of Thermal Sciences, 50, 712-717 (2011).

Nassan, T. H., Heris, S. Z., Noie, S. H., A comparison of experimental heat transfer characteristics for Al_2O_3/water and CuO/water nanofluids in square cross-section duct. International Communications in Heat and Mass Transfer, 37, 924-928 (2010).

Nield, D. A., Kuznetsov, A. V., The Cheng-Minkowycz problem for natural convective boundary-layer flow in a porous medium saturated by a nanofluid. International Journal of Heat and Mass Transfer, 52, 5792-5795 (2009).

Noghrehabadi, A., Ghalambaz, M., Ghanbarzadeh, A., Comparing thermal enhancement of Ag-water and SiO_2-water nanofluids over an isothermal stretching sheet with suction or injection. Journal of Computational and Applied Research in Mechanical Engineering, 2, 35-47 (2012a).

Noghrehabadi, A., Ghalambaz, M., Ghanbarzadeh, A., Heat transfer of magnetohydrodynamic viscous nanofluids over an isothermal stretching sheet. Journal of Thermophysics and Heat Transfer, 26, 686-689 (2012b).

Noghrehabadi, A., Pourrajab, R., Ghalambaz, M., Effect of partial slip boundary condition on the flow and heat transfer of nanofluids past stretching sheet prescribed constant wall temperature. International Journal of Thermal Sciences, 54, 253-261 (2012c).

Noghrehabadi, A., Pourrajab, R., Ghalambaz, M., Flow and heat transfer of nanofluids over stretching sheet taking into account partial slip and thermal convective boundary conditions. Heat Mass Transfer, 49, 1357-1366 (2013a).

Noghrehabadi, A., Saffarian, M. R., Pourrajab, R., Ghalambaz, M., Entropy analysis for nanofluid flow over a stretching sheet in the presence of heat generation/absorption and partial slip. Journal of Mechanical Science and Technology, 27, 927-937 (2013b).

Noghrehabadi, A., Behseresht, A., Ghalambaz, M., Behseresht, J., Natural-convection flow of nanofluids over vertical cone embedded in non-Darcy porous media. Journal of Thermophysics and Heat Transfer, 27, 334-341 (2013c).

Noghrehabadi, A., Behseresht, A., Ghalambaz, M., Natural convection of nanofluid over vertical plate embedded in porous medium: Prescribed surface heat flux. Applied Mathematics and Mechanics, 34(6), 669-686 (2013d).

Nnanna, A. G., Experimental model of temperature-driven nanofluid. ASME Transactions Journal of Heat Transfer, 129, 697-704 (2007).

Polidori, G., Fohanno, S., Nguyen, C. T., A note on heat transfer modeling of Newtonian nanofluids

in laminar free convection. International Journal of Thermal Sciences, 46, 739-744 (2007).
Putra, N., Roetzel, W., Das, S. K., Natural convection of nano-fluids. Heat and Mass Transfer, 39, 775-784 (2003).
Rashad, A. M., El-Hakiem, M. A., Abdou, M. M. M., Natural convection boundary layer of a non-Newtonian fluid about a permeable vertical cone embedded in a porous medium saturated with a nanofluid. Computers & Mathematics with Applications, 62, 3140-3151 (2011).
Vajravelu, K., Prasad, KV., Lee, J., Lee, C., Pop, I., Van Gorder, R. A., Convective heat transfer in the flow of viscous Ag–water and Cu–water nanofluids over a stretching surface. International Journal of Thermal Sciences, 50, 843-851 (2011).
Wang, X.-Q, Mujumdar, A. S., A review on nanofluids - Part I: Theoretical and numerical investigations. Braz. J. Chem. Eng., 25, 613-630 (2008a).
Wang, X.-Q, Mujumdar, A. S., A review on nanofluids - Part II: Experiments and applications. Braz. J. Chem. Eng., 25, 631-648 (2008b).
Wen, D., Ding, Y., Natural convective heat transfer of suspensions of titanium dioxide nanoparticles (nanofluids). IEEE Transactions on Nanotechnology, 5, 220-227 (2006).
Wongcharee, K., Eiamsa-Ard, S., Enhancement of heat transfer using CuO/water nanofluid and twisted tape with alternate axis. International Communications in Heat and Mass Transfer, 38(6), 742-748 (2011).
Yacob, N. A., Ishak, A., Nazar, R., Pop, I., Falkner–Skan problem for a static and moving wedge with prescribed surface heat flux in a nanofluid. International Communications in Heat and Mass Transfer, 38(2), 149-153 (2011a).
Yacob, N. A., Ishak, A., Pop, I., Vajravelu, K., Boundary layer flow past a stretching/shrinking surface beneath an external uniform shear flow with a convective surface boundary condition in a nanofluid. Nanoscale Research Letters, 6(1), 1-7 (2011b).
Yu, W., France, D. M., Routbort, J. L., Choi, S. U., Review and comparison of nanofluid thermal conductivity and heat transfer enhancements. Heat Transfer Engineering, 29(5), 432-460 (2008).
Zheng, F., Thermophoresis of spherical and non-spherical particles: A review of theories and experiments. Advances in Colloid and Interface Science, 97, 255-278 (2002).

APPENDIX

Using cross-differentiation and the definition of the stream function, Eq. (8), the momentum equation, Eqs. (2a) and (2b), are simplified as,

$$\frac{\partial^2 \psi}{\partial y^2} = \frac{(1-\phi_\infty)\rho_{f\infty}\beta g \kappa}{\mu}\frac{\partial T}{\partial y} - \frac{(\rho_p - \rho_{f\infty})g\kappa}{\mu}\frac{\partial \phi}{\partial y} \quad \text{(A1)}$$

Here, by using the introduced similarity variables, Eqs. (10) and (11), each term of Eq. (A1) can be written as follows,

$$\frac{\partial \eta}{\partial y} = \frac{Ra_x^{\frac{1}{2}}}{x} \quad \text{(A2)}$$

$$\frac{\partial \psi}{\partial S} = \alpha_m Ra_x^{\frac{1}{2}} \quad \text{(A3)}$$

$$\frac{\partial \psi}{\partial y} = \frac{\partial \psi}{\partial S}\frac{\partial S}{\partial \eta}\frac{\partial \eta}{\partial y} = \alpha_m \frac{Ra_x}{x} S' \quad \text{(A4)}$$

$$\frac{\partial^2 \psi}{\partial y^2} = \left(\alpha_m \frac{Ra_x^{\frac{3}{2}}}{x^2}\right) S'' \quad \text{(A5)}$$

$$\frac{\partial T}{\partial y} = \frac{\partial T}{\partial \theta}\frac{\partial \theta}{\partial \eta}\frac{\partial \eta}{\partial y} = (T_f - T_\infty)\left(\frac{Ra_x^{\frac{1}{2}}}{x}\right)\theta' \quad \text{(A6)}$$

$$\frac{\partial \phi}{\partial y} = \frac{\partial \phi}{\partial f}\frac{\partial f}{\partial \eta}\frac{\partial \eta}{\partial y} = (\phi_w - \phi_\infty)\frac{Ra_x^{\frac{1}{2}}}{x} f' \quad \text{(A7)}$$

Substituting Eqs. (A5)-(A7) into (A1), the following equation is obtained,

$$\left(\alpha_m \frac{Ra_x^{\frac{3}{2}}}{x^2}\right) S'' = \frac{(1-\phi_\infty)\rho_{f\infty}\beta g\kappa}{\mu}\left[(T_f - T_\infty)\left(\frac{Ra_x^{\frac{1}{2}}}{x}\right)\theta'\right] - \frac{(\rho_p - \rho_{f\infty})g\kappa}{\mu}\left[(\phi_w - \phi_\infty)\frac{Ra_x^{\frac{1}{2}}}{x} f'\right] \quad \text{(A8)}$$

Where, by dividing by $\alpha_m \frac{Ra_x^{\frac{3}{2}}}{x^2}$, it can be simplified as follows:

$$S'' = \theta' - \frac{(\rho_p - \rho_{f\infty})(\phi_w - \phi_\infty)}{(1-\phi_\infty)\rho_{f\infty}\beta(T_f - T_\infty)} f' \quad \text{(A9)}$$

$$S'' - \theta' + Nr.f' = 0 \quad \text{(A10)}$$

where:

$$Nr = \frac{(\rho_p - \rho_{f\infty})(\phi_w - \phi_\infty)}{(1-\phi_\infty)\rho_{f\infty}\beta(T_f - T_\infty)} \quad \text{(A11)}$$

Using the similarity variables, Eqs. (10) and (11), each term of the energy equation, Eq. (3), can be evaluated as follows,

$$\frac{\partial \eta}{\partial x} = \left(\frac{-1}{2}\right) y \frac{Ra_x^{\frac{1}{2}}}{x^2} \quad \text{(A12)}$$

$$\frac{\partial T}{\partial x} = \frac{\partial T}{\partial \theta}\frac{\partial \theta}{\partial \eta}\frac{\partial \eta}{\partial x} = (T_f - T_\infty)\left(\left(\frac{-1}{2}\right) y \frac{Ra^{\frac{1}{2}}}{x^2}\right)\theta' \quad \text{(A13)}$$

$$\frac{\partial \psi}{\partial x} = S.\frac{\partial}{\partial x}\left(\alpha_m Ra_x^{\frac{1}{2}}\right) + \left(\alpha_m Ra_x^{\frac{1}{2}}\right).\frac{\partial S}{\partial \eta}\frac{\partial \eta}{\partial x}$$
$$= \frac{1}{2}\alpha_m \frac{Ra_x^{\frac{1}{2}}}{x} S + \left(\alpha_m Ra_x^{\frac{1}{2}}\right)\left(\frac{-1}{2} y \frac{Ra_x^{\frac{1}{2}}}{x^2}\right) S' \quad \text{(A14)}$$
$$= \frac{1}{2}\alpha_m \frac{Ra_x^{\frac{1}{2}}}{x} S - \frac{1}{2}\alpha_m y \frac{Ra_x}{x^2} S'$$

$$\frac{\partial^2 T}{\partial y^2} = (T_f - T_\infty)\left(\frac{Ra_x}{x^2}\right)\theta'' \quad \text{(A15)}$$

$$\left(\frac{\partial T}{\partial y}\right)^2 = (T_f - T_\infty)^2\left(\frac{Ra_x}{x^2}\right)\theta'^2 \quad \text{(A16)}$$

Substituting Eqs. (A4), (A6)-(A7) and (A13)-(A16) into Eq. (12), the following equation is obtained,

$$\left(\alpha_m \frac{Ra_x}{x} S'\right)\left(\frac{-1}{2} y \frac{Ra_x^{\frac{1}{2}}}{x^2}(T_f - T_\infty)\theta'\right) - \left(\frac{1}{2}\alpha_m \frac{Ra_x^{\frac{1}{2}}}{x} S - \frac{1}{2}\alpha_m y \frac{Ra_x}{x^2} S'\right) \times \left((T_f - T_\infty)\left(\frac{Ra_x^{\frac{1}{2}}}{x}\right)\theta'\right)$$
$$= \alpha_m (T_f - T_\infty)\left(\frac{Ra_x}{x^2}\right)\theta'' + \tau\left[D_B\left((\phi_w - \phi_\infty)\frac{Ra_x^{\frac{1}{2}}}{x} f'\right)\left((T_f - T_\infty)\left(\frac{Ra_x^{\frac{1}{2}}}{x}\right)\theta'\right) + \frac{D_T}{T_\infty}\left((T_f - T_\infty)^2\left(\frac{Ra_x}{x^2}\right)\theta'^2\right)\right] \quad \text{(A17)}$$

Where, by dividing by $\alpha_m (T_f - T_\infty)\frac{Ra_x}{x^2}$, it can be simplified as follows:

$$-\frac{1}{2} S\theta' = \theta'' + \tau\left[\frac{D_B(\phi_w - \phi_\infty)}{\alpha_m} f'\theta' + \frac{D_T(T_f - T_\infty)}{T_\infty \alpha_m}\theta'^2\right] \quad \text{(A18)}$$

$$\theta'' + \frac{1}{2} S\theta' + Nb.f'\theta' + Nt.\theta'^2 = 0 \tag{A19}$$

where:

$$Nb = \frac{\varepsilon(\rho c)_p D_B(\phi_w - \phi_\infty)}{(\rho c)_f \alpha_m}, \qquad Nt = \frac{\varepsilon(\rho c)_p D_T(T_f - T_\infty)}{(\rho c)_f \alpha_m T_\infty} \tag{A20}$$

The two terms of conservation of nanoparticle, Eq. (4), can be evaluated as follows:

$$\frac{\partial^2 \phi}{\partial y^2} = (\phi_w - \phi_\infty)\frac{Ra_x}{x^2} f'' \tag{A21}$$

$$\frac{\partial \phi}{\partial x} = \frac{\partial \phi}{\partial f}\frac{\partial f}{\partial \eta}\frac{\partial \eta}{\partial x} = (\phi_w - \phi_\infty)\left(\frac{-1}{2} y \frac{Ra_x^{\frac{1}{2}}}{x^2}\right) f' \tag{A22}$$

Substituting Eqs. (A4), (A7), (A14)-(A15) and (A21)-(A22) into Eq. (12), the following equation is obtained:

$$\frac{1}{\varepsilon}\left[\left(\alpha_m \frac{Ra}{x} S'\right)\times\left((\phi_w - \phi_\infty)\left(\frac{-1}{2} y \frac{Ra_x^{\frac{1}{2}}}{x^2}\right) f'\right)\right.$$
$$-\left(\frac{1}{2}\alpha_m \frac{Ra_x^{\frac{1}{2}}}{x} S + \left(\alpha_m Ra^{\frac{1}{2}}\right)\left(\frac{-1}{2} y \frac{Ra^{\frac{1}{2}}}{x^2}\right) S'\right) \tag{A23}$$
$$\left.\times(\phi_w - \phi_\infty)\frac{Ra^{\frac{1}{2}}}{x} f'\right] = D_B\left((\phi_w - \phi_\infty)\frac{Ra}{x^2} f''\right)$$
$$+\frac{D_T}{T_\infty}\left((T_f - T_\infty)\left(\frac{Ra}{x^2}\right)\theta''\right)$$

Where, by dividing by $D_B(\phi_w - \phi_\infty)\frac{Ra}{x^2}$, it can be simplified as follows,

$$-\frac{1}{2}\frac{\alpha_m}{\varepsilon D_B} Sf' = f'' + \frac{D_T(T_f - T_\infty)}{T_\infty D_B(\phi_w - \phi_\infty)}\theta'' \tag{A24}$$

$$f'' + \frac{1}{2} Le.Sf' + \frac{Nt}{Nb}\theta'' = 0 \tag{A25}$$

where:

$$\frac{Nt}{Nb} = \frac{D_T(T_f - T_\infty)}{T_\infty D_B(\phi_w - \phi_\infty)}, Le = \frac{\alpha_m}{\varepsilon D_B} \tag{A26}$$

Substituting Eq. (A6) in the equation for the convective heating boundary condition, Eq. (15), and using the similarity variable of the temperature, Eq. (11), the following equation is obtained:

$$-k(T_f - T_\infty)\left(\frac{Ra_x^{\frac{1}{2}}}{x}\right)\theta'(0) = h_f\left[T_f - \left((T_f - T_\infty)\theta(0) + T_\infty\right)\right] \tag{A27}$$

Simplifying Eq. (A27) leads to,

$$\theta'(0) = \frac{h_f x^{\frac{1}{2}}}{k\left(\frac{(1-\phi_\infty)\beta\kappa g(T_f - T_\infty)}{\mu\alpha}\right)^{\frac{1}{2}}}\left[1 - \theta(0)\right] \tag{A28}$$

$$\theta'(0) = Nc\left[1 - \theta(0)\right] \tag{A29}$$

where,

$$Nc = \frac{h_f x^{\frac{1}{2}}}{k\left(\frac{(1-\phi_\infty)\beta\kappa g(T_f - T_\infty)}{\mu\alpha}\right)^{\frac{1}{2}}} \tag{A30}$$